JACC: CARDIOVASCULAR INTERVENTIONS VOL. 11, NO. 20, 2018

PUBLISHED BY ELSEVIER

# Low Coronary Wall Shear Stress Is Associated With Severe Endothelial Dysfunction in Patients With Nonobstructive Coronary Artery Disease

Arnav Kumar, MD,[a] Olivia Y. Hung, MD, PhD,[a] Marina Piccinelli, PhD,[b] Parham Eshtehardi, MD,[a] Michel T. Corban, MD,[c] David Sternheim, MD,[a] Boyi Yang, PhD,[d] Adrien Lefieux, PhD,[a,d] David S. Molony, PhD,[a] Elizabeth W. Thompson, BS,[a] Wenjie Zeng, MD, MPH,[a] Yasir Bouchi, BS,[a] Sonu Gupta, MD,[a] Hossein Hosseini, MD,[a] Mohamad Raad, MD,[a] Yi-An Ko, PhD,[e] Chang Liu, MPH,[a] Michael C. McDaniel, MD,[a] Bill D. Gogas, MD, PhD,[a] John S. Douglas, MD,[a] Arshed A. Quyyumi, MD,[a] Don P. Giddens, PhD,[f] Alessandro Veneziani, PhD,[d] Habib Samady, MD[a]

## ABSTRACT

**OBJECTIVES** This study investigated the relationship between low wall shear stress (WSS) and severe endothelial dysfunction (EDFx).

**BACKGROUND** Local hemodynamic forces such as WSS play an important role in atherogenesis through their effect on endothelial cells. The study hypothesized that low WSS independently predicts severe EDFx in patients with coronary artery disease (CAD).

**METHODS** Forty-four patients with CAD underwent coronary angiography, fractional flow reserve, and endothelial function testing. Segments with >10% vasoconstriction after acetylcholine (Ach) infusion were defined as having severe EDFx. WSS, calculated using 3-dimensional angiography, velocity measurements, and computational fluid dynamics, was defined as low (<1 Pa), intermediate (1 to 2.5 Pa), or high (>2.5 Pa).

**RESULTS** Median age was 52 years, 73% were women. Mean fractional flow reserve was 0.94 ± 0.06. In 4,510 coronary segments, median WSS was 3.67 Pa. A total of 24% had severe EDFx. A higher proportion of segments with low WSS had severe EDFx (71%) compared with intermediate WSS (22%) or high WSS (23%) ($p < 0.001$). Segments with low WSS demonstrated greater vasoconstriction in response to Ach than did intermediate or high WSS segments (−10.7% vs. −2.5% vs. +1.3%, respectively; $p < 0.001$). In a multivariable logistic regression analysis, female sex (odds ratio [OR]: 2.44; $p = 0.04$), diabetes (OR: 5.01; $p = 0.007$), and low WSS (OR: 9.14; $p < 0.001$) were independent predictors of severe EDFx.

**CONCLUSIONS** In patients with nonobstructive CAD, segments with low WSS demonstrated more vasoconstriction in response to Ach than did intermediate or high WSS segments. Low WSS was independently associated with severe EDFx. (J Am Coll Cardiol Intv 2018;11:2072–80) © 2018 by the American College of Cardiology Foundation.

From the [a]Andreas Gruentzig Cardiovascular Center, Division of Cardiology, Department of Medicine, Emory University School of Medicine, Atlanta, Georgia; [b]Department of Radiology, Emory University School of Medicine, Atlanta, Georgia; [c]Department of Cardiovascular Diseases, Mayo Clinic College of Medicine and Science, Rochester, Minnesota; [d]Department of Mathematics and Computer Science, Emory University, Atlanta, Georgia; [e]Department of Biostatistics and Bioinformatics, Rollins School of Public Health, Emory University, Atlanta, Georgia; and the [f]Wallace H. Coulter Department of Biomedical Engineering, Georgia Institute of Technology and Emory University, Atlanta, Georgia. This study was funded by the Wallace H. Coulter Translational/Clinical Research Seed Grant Program of Georgia Institute of Technology, Emory University, and Volcano Corporation; and supported in part by Public Health Service Grant No. UL1 RR025008 from the Clinical and Translational Science Award program, National Institutes of Health, National Center for Research Resources. Drs. Hung and Eshtehardi were supported by a Ruth L. Kirschstein National Research Service Awards training grant (no. 5T32HL007745). Dr. Samady has received research grants from Abbott Vascular, Medtronic, National Institutes of Health, St. Jude Medical, and Gilead; and owns

ISSN 1936-8798/$36.00 https://doi.org/10.1016/j.jcin.2018.07.004

Atherosclerosis is a systemic disease with focal manifestations often initiating in the outer hips of bifurcations and inner curvatures of vessels. Local hemodynamic forces, such as wall shear stress (WSS), play an important role in atherogenesis, likely mediated through endothelial cells. WSS, the tangential frictional force exerted by blood flow on the arterial wall, has been associated with atherosclerotic plaque progression in human coronary arteries (1-7). Endothelial dysfunction (EDFx) occurs early in the development of atherosclerosis and is believed to be the final common pathway by which systemic risk factors have an impact on the vasculature (8,9). Moreover, EDFx is characterized by a local imbalance between atheroprotective endothelium-dependent vasodilators such as nitric oxide and proinflammatory, proliferative, and procoagulopathic endothelium-derived vasoconstrictive

SEE PAGE 2081

factors that favor atherogenesis (10). Interestingly, regional coronary arterial endothelial responses to acetylcholine (Ach) are heterogeneous in the same patient despite exposure of the entire vessel to the same systemic risk factors (9,11,12). This focal variability in EDFx may be related to differences in WSS. Arterial endothelial cell alignment is known to follow WSS direction and low WSS has been theorized to cause EDFx by altering the activity of several inflammatory pathways (13). To date the role of WSS in promoting EDFx in vivo has not been fully characterized. We hypothesized that in patients with nonobstructive coronary artery disease (CAD), coronary segments with low WSS demonstrate greater EDFx compared with segments with intermediate or high WSS. Accordingly, we investigated the relationship between WSS and EDFx in patients with nonobstructive CAD using a 3-dimensional angiographic reconstruction and patient specific coronary velocity measurements to derive computational fluid dynamics computations of WSS.

## METHODS

**SUBJECTS AND STUDY DESIGN.** We selected all patients who were enrolled in our prospective Emory intravascular registry between August 2012 and October 2014. The Emory intravascular registry consists of patients who had an abnormal noninvasive stress test or presented with refractory anginal syndromes, underwent cardiac catheterization, were found to have nonobstructive epicardial coronary atherosclerotic lesions (fractional flow reserve >0.80), and underwent further coronary reactivity testing with intracoronary Ach infusion. Exclusion criteria included acute myocardial infarction with cardiogenic shock or hemodynamic instability, ejection fraction <30%, coronary artery bypass surgery, severe valvular heart disease, lesions requiring percutaneous or surgical revascularization, presence of visual coronary collateral vessels, inability to provide informed consent, or significant kidney (creatinine >1.5 mg/dl) or liver disease (aspartate aminotransferase, alanine aminotransferase, or alkaline phosphatase higher than 3 times the normal limit). We also excluded patients with hemoglobin <7 g/dl, platelet count <100 K/μl, or international normalized ratio >1.5. For the present analysis, in addition to the clinical exclusion criteria, patients who did not have sufficiently high-quality baseline and post-Ach angiograms for accurate 3-dimensional (3D) reconstruction for purposes of WSS calculations and endothelial function assessment were also excluded. All patients provided written informed consent and the Emory University Institutional Review Board approved the study.

**CORONARY ANGIOGRAPHY, CORONARY VELOCITY MEASUREMENT WITH ENDOTHELIAL FUNCTION ASSESSMENT.** As described previously (1,2,5,14), all vasoactive medications were held for at least 24 to 48 h before cardiac catheterization. Systolic blood pressure, diastolic blood pressure, and heart rate were measured before the start of the procedure. Patients underwent angiography in a biplane cardiac catheterization system (Philips Medical Systems, Andover, Massachusetts; or Toshiba America Medical Systems, Tustin, California). Pressure and velocity measurements were obtained using a 0.014-inch pressure and Doppler flow velocity monitoring guidewire (ComboWire, Volcano Corporation, Rancho Cordova, California). The ComboWire was advanced to the guide catheter tip where the aortic pressure and guidewire pressures were equalized. The guidewire was advanced into the proximal, nontortuous portion of the left anterior descending coronary artery or left circumflex artery (based on

**ABBREVIATIONS AND ACRONYMS**

**3D** = 3-dimensional
**Ach** = acetylcholine
**CAD** = coronary artery disease
**CFR** = coronary flow velocity reserve
**EDFx** = endothelial dysfunction
**IQR** = interquartile range
**OR** = odds ratio
**QCA** = quantitative coronary angiography
**WSS** = wall shear stress
**%ΔD** = percent change in vessel diameter in response to acetylcholine

stock in Covanos and Sidney Investment Group. All other authors have reported that they have no relationships relevant to the contents of this paper to disclose.

Manuscript received April 30, 2018; revised manuscript received July 2, 2018, accepted July 3, 2018.

**FIGURE 1 Three-Dimensional Geometric Reconstruction Showing 0.5-mm Segmentation and Calculated Segment-Level WSS**

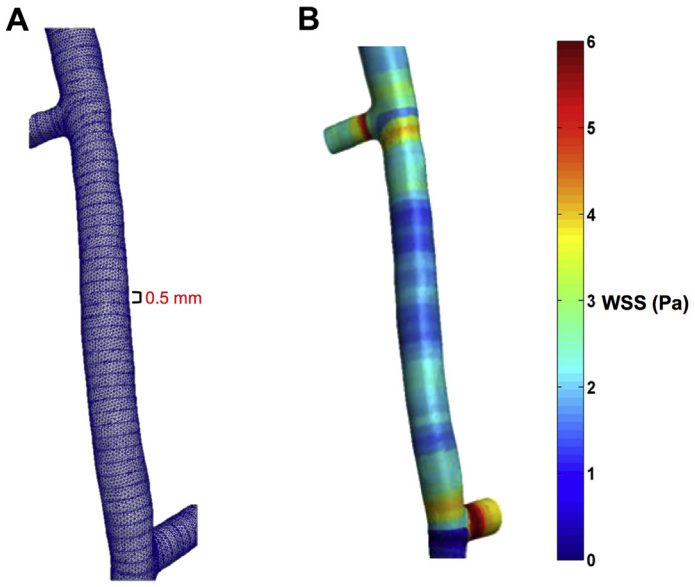


**(A)** Biplane angiographic projections were used to create a 3-dimensional model of the target coronary vessel, which was subsequently divided into 0.5-mm longitudinal segments (seen as circumferential bands) and meshed using automated software. **(B)** After performing computational fluid dynamics with patient-specific boundary conditions, wall shear stress (WSS) was averaged across each 0.5-mm segment; the resulting values are displayed as 0.5-mm color-coded bands representing the calculated average WSS per segment.

operator discretion) at least 5 mm from major angiographic side branches (>2-mm diameter) and the inlet velocity was recorded. The ComboWire was then advanced into the mid or distal artery and the outlet velocity and pressure was recorded. Patients were first evaluated with $10^{-8}$ M Ach for safety before proceeding with $10^{-6}$ M Ach (18.2 μg/ml at the rate of 90 ml/h infused intracoronary through a 3-F microcatheter over 3 min). Biplane coronary angiography was performed after each infusion to assess vascular response. Patients were not moved or repositioned in between serial coronary angiograms. The same radiographic system, magnification, and views were used for the serial angiograms. Intravenous nitroglycerin (200 μg) was then given to reverse residual vasoconstrictive effects and angiography repeated. Subsequently, 140 μg/kg/min adenosine was infused through a ≥20-gauge intravenous catheter for 2 min to induce maximal coronary hyperemia. Continuous recordings of aortic pressure, distal pressure, and velocity were obtained during baseline and drug infusion periods. During maximal hyperemia, fractional flow reserve was defined as the ratio of mean distal to aortic pressure and coronary flow velocity reserve was defined as the ratio of hyperemic to basal average peak velocity. Velocity measurements demonstrated good reproducibility with a concordance correlation coefficient of 0.979 (95% confidence interval: 0.966 to 0.988) (1).

**ENDOTHELIAL FUNCTION, COMPUTATIONAL FLUID DYNAMICS, AND WSS METHODOLOGY AND CALCULATIONS.** Three-dimensional geometric reconstructions of each patient's target vessel were performed offline on pre- and post-Ach cineangiograms using QAngio XA 3D RE (Medis Medical Imaging Systems, Leiden, the Netherlands). All visible branching vessels were included in the 3D reconstruction. The pre- and post-Ach reconstructions were coregistered using branching points as fiduciary anatomical landmarks. The resulting pre- and post-Ach 3D models were analyzed by means of fully automated software tools for the extraction of centerlines, computation of pointwise radius map, and the discretization of each vessel in longitudinal segments of 0.5-mm length (**Figure 1A**) (see Online Appendix) (15,16). Percent change in diameter (%ΔD) was calculated for each 0.5-mm segment as $100\% \times (D_{post} - D_{pre}) / D_{pre}$. Based on prior studies, each coronary segment demonstrating %ΔD >−10% was defined as having severe EDFx (17-21). Similarly, segments with %ΔD between −10% to +10% in response to Ach were defined as having mild EDFx, whereas those with %ΔD ≥+10% were defined as having normal endothelial function. After the reconstructed baseline 3D surface was meshed, computational fluid dynamics was carried out using the finite element library LifeV (EPFL, Lausanne, Switzerland; Politecnico di Milano, Milan, Italy; French Institute for Research in Computer Science and Automation, Rocquencourt, France; and Emory University, Atlanta, Georgia). Post-processing was carried out by the open source software Paraview 5.4 (Kitware, Clifton Park, New York). The fluid (blood) was assumed to be a homogeneous pulsatile isothermal incompressible Newtonian fluid (viscosity constant with respect to shear rate) (22), allowing for the use of the incompressible Navier-Stokes equations that can be numerically solved by applying the finite element method (23). Three cardiac cycles were simulated to reach the desired pulsatile regime with satisfactory accuracy in the velocity field. Boundary conditions of the target vessel and its branches were specified as a series of velocity and pressure profiles measured by the ComboWire in conjunction with an application of Murray's law (24,25) that weighs the flux of each

arterial branch, including the distal portion of the target vessel, with respect to its neighbor. This has been demonstrated to be a reasonable mathematical assumption for mildly stenotic coronaries, as in the present study (26). Spatial velocity profiles were assumed to be flat in the 80% inner part of the proximal vessel, with a linear decrease in the profile in the outermost part of the proximal vessel (to satisfy the no-slip boundary condition on the wall), and parabolic in the arterial branch outlets. After computing the pulsatile flow field in the region of interest, the WSS map was determined on the vessel surface as a function of time in the cardiac cycle (27,28), then averaged over time and circumference at each 0.5-mm segment for quantitative analysis (**Figure 1B**). Based on previous experimental and human data, low WSS was categorized as <1 Pa (1,2,5,29-31). Intermediate WSS was categorized as ≥1 Pa but <2.5 Pa, whereas high WSS was defined as ≥2.5 Pa.

**STATISTICAL ANALYSIS.** Continuous variables are summarized as mean ± SD or median (interquartile range [IQR]), as appropriate, and categorical variables as count and proportion. The association between WSS and severe EDFx was investigated using logistic regression models. To account for the correlations within patient due to repeated measurements (segments), a robust "sandwich" variance estimator was used to estimate the variance-covariance matrix of the regression parameter coefficients by generalized estimating equations. An independence working correlation structure was chosen based on the QIC (quasi-likelihood under the independence model criterions) statistic. The covariates included age, sex, race (African American vs. non-African American), diabetes mellitus (glycosylated hemoglobin >7%), hypertension (systolic blood pressure >140 mm Hg or diastolic blood pressure >90 mm Hg), hyperlipidemia (low-density lipoprotein >100 mg/dl), and active smoking (yes vs. no). Subsequently, a linear regression model was used to investigate the relationship between WSS and %ΔD, again with generalized estimating equations to account for within-subject correlations, and adjusted for the aforementioned covariates. In these models, WSS was treated as a binary variable (<1 Pa vs. ≥1 Pa) and then a continuous variable (measured in Pascals). In addition, a generalized additive mixed model was used to explore the relationship between WSS and severe EDFx (with logit link). The model was fit by a smooth term of WSS using a cubic spline smoothing with a basis dimension of 3. A p value < 0.05 was considered statistically significant. Analyses were performed using SAS 9.4 (SAS Institute, Cary, North Carolina), R version 3.4.1 (R Foundation for Statistical Computing, Vienna, Austria), and SPSS 24.0 (IBM Corporation, Armonk, New York).

**TABLE 1 Demographic and Clinical Characteristics of Study Patients (N = 44)**

| | |
|---|---|
| Age (yrs) | 52.0 (44.0-66.0) |
| Female | 32 (73) |
| African American | 24 (55) |
| Cardiovascular risk factors | |
| Hypertension | 13 (30) |
| Diabetes mellitus | 1 (2) |
| Hyperlipidemia | 20 (45) |
| Current smoker | 3 (7) |
| Medication use | |
| Aspirin | 23 (52) |
| $P2Y_{12}$ inhibitor | 5 (11) |
| Statin | 20 (45) |
| Beta-blocker | 16 (36) |
| Calcium-channel blocker | 9 (20) |
| Long-acting nitrate | 10 (23) |
| ACE inhibitor or ARB | 10 (23) |

Values are median (interquartile range) or n (%).
ACE = angiotensin-converting enzyme; ARB = angiotensin receptor blocker.

## RESULTS

We evaluated 44 coronary arteries (93% left anterior descending artery) in 44 patients. Baseline demographics and clinical characteristics of the study cohort are shown in **Table 1**. Median age of the study population was 52.0 (IQR: 44.0 to 66.0) years and 73% of patients were women. Median angiographic diameter stenosis was 18.3% (IQR: 13.6% to 26.5%). Median fractional flow reserve was 0.95 (IQR: 0.91 to 0.99) and median coronary flow velocity reserve was 2.2 (IQR: 1.8 to 2.5). Overall, 4,510 vessel segments (each 0.5 mm in length, a total of 2,255 mm) were analyzed. Median segmental baseline diameter was 2.3 (IQR: 1.9 to 2.7) mm. Median post-Ach diameter was 2.3 (IQR: 1.9 to 2.7) mm, whereas median %ΔD was 0% (IQR: −9.0% to 10.0%).

Among 4,510 analyzed vessel segments, median WSS was 3.67 (IQR: 2.39 to 5.53) Pa. Low, intermediate, and high WSS were found in 110 (2.4%), 1,117 (24.8%), and 3,283 (72.8%) segments, respectively. Normal endothelial function was observed in 1,171 (26%) segments, mild EDFx in 2,273 (50.4%)

**FIGURE 2 Boxplots of Percent Change in Diameter in Response to Acetylcholine in Segments With Low, Intermediate, and High Segmental WSS**

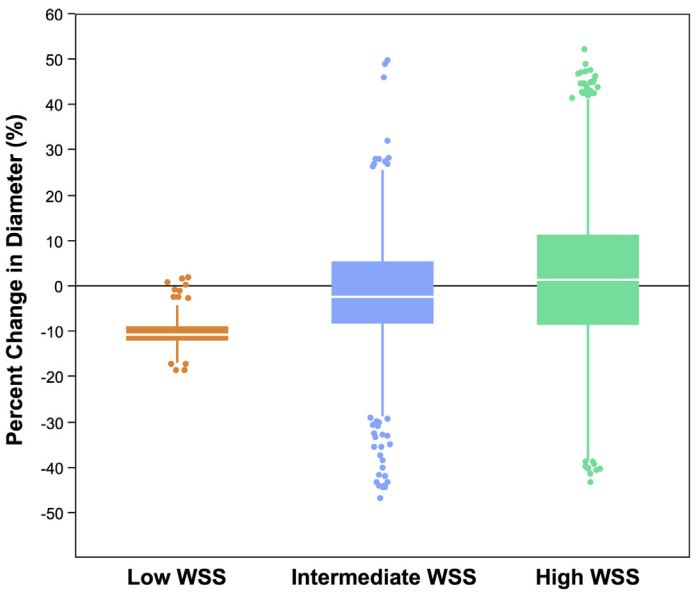


The **line subdividing the box** represents the median. Error bars are drawn to span all data points within 1.5 interquartile range of the nearer quartile. Any data points beyond 1.5 interquartile range are shown individually. Both high-WSS (n = 3,283) and intermediate-WSS (n = 1,117) segments demonstrated higher percent change in diameter when compared with low-WSS segments (n = 110) after adjusting for within-subject correlations using generalized estimating equations ($p < 0.001$). Abbreviation as in Figure 1.

segments, and severe EDFx in 1,066 (23.6%) segments.

**SEGMENT LEVEL RELATIONSHIP BETWEEN ENDOTHELIAL FUNCTION AND WSS.** After accounting for within subject correlation, segments with low WSS demonstrated greater vasoconstriction in response to Ach than did segments with intermediate or high WSS (−10.7% [IQR: −12.1% to −8.8%] vs. −2.5% [IQR: −8.3% to +5.5%] vs. +1.3% [IQR: −8.6% to +11.3%], respectively; $p < 0.001$) (Figure 2). Furthermore, low WSS was associated with a mean −0.11 %ΔD in response to Ach ($p < 0.001$) after adjusting for various demographic and cardiovascular risk factors (Table 2).

A higher proportion of segments with low WSS had severe EDFx (71%), compared with intermediate WSS (22%) or high WSS (23%) ($p < 0.001$) (Figure 3). Interestingly, no segment with normal endothelial function had low WSS. In a univariable logistic regression analysis, low WSS was associated with severe EDFx (odds ratio [OR]: 8.42; $p < 0.001$]. In a multivariable logistic regression model, female sex (OR: 2.44; $p = 0.04$), diabetes (OR: 5.01; $p = 0.007$), and low WSS (OR: 9.14; $p < 0.001$) were independent predictors of severe EDFx (Table 3). Figure 4A shows a representative coronary vessel with numerous low-WSS segments and Figure 4B shows the corresponding distribution of endothelial function in the same vessel. Notice the high number of segments with severe or mild EDFx colocalized with low-WSS areas. Figure 5 shows the estimated probability of severe EDFx as a function of WSS between 0 and 10 Pa. The estimated probability of severe EDFx increases from 0.50 (50%) to 0.95 (95%) as WSS decreases from 4 to 1 Pa.

**TABLE 2 Associations Between %ΔD and Low Wall Shear Stress Using Linear Regression With Generalized Estimating Equations to Account for Within-Subject Correlations**

| | Univariate Models | | Multivariable Model | |
|---|---|---|---|---|
| | Estimated Difference in %ΔD (95% CI) | p Value | Estimated Difference in %ΔD (95% CI) | p Value |
| Age (yrs) | −0.0003 (−0.003 to 0.002) | 0.81 | 0.01 (−0.01 to 0.01) | 0.38 |
| Female | −0.069 (−0.138 to 0.0004) | 0.05 | −0.07 (−0.13 to −0.01) | 0.03 |
| African American | −0.002 (−0.064 to 0.059) | 0.95 | 0.03 (−0.05 to 0.07) | 0.74 |
| Hypertension | −0.013 (−0.084 to 0.058) | 0.71 | −0.01 (−0.09 to −0.06) | 0.70 |
| Diabetes mellitus | −0.145 (−0.178 to 0.112) | <0.001 | −0.22 (−0.22 to −0.09) | <0.001 |
| Active smoker | −0.041 (−0.110 to 0.028) | 0.24 | −0.05 (−0.13 to −0.037) | 0.28 |
| Hyperlipidemia | −0.006 (−0.074 to 0.062) | 0.87 | −0.015 (−0.08 to −0.05) | 0.64 |
| Low wall shear stress | −0.110 (−0.142 to 0.077) | <0.001 | −0.11 (−0.18 to −0.047) | <0.001 |

CI = confidence interval; %ΔD = diameter change in response to acetylcholine.

## DISCUSSION

This clinical study investigates the relationship between time-averaged WSS and coronary endothelial function derived from baseline and post-Ach 3D coronary angiography in patients with nonobstructive CAD. The results demonstrate that in patients with nonobstructive CAD: 1) coronary segments with low WSS show a higher degree of vasoconstriction and severe EDFx compared with segments with intermediate or high WSS; 2) low WSS is independently associated with severe EDFx; and 3) the estimated probability of severe EDFx increases at lower WSS values and reaches its highest peak at <1 Pa.

**MECHANISMS OF WSS AND EDFx: FROM BENCH TO BEDSIDE.** There is a growing body of molecular data linking low WSS to the development of EDFx. Experimental ex vivo studies have demonstrated multiple mechanisms by which low WSS induces changes in endothelial cell morphology with loss of alignment and increased turnover (32-34). Sustained low WSS affects the structure and function of endothelial cells, resulting in transformation to a

proatherogenic phenotype with polygonal morphology (32,34,35). Moreover, low WSS down-regulates the expression of endothelial nitric oxide synthase (36-38), which generates nitric oxide and plays a crucial role in maintaining coronary arterial vasodilation. The loss of endothelial nitric oxide synthase, and decreased NO production, leads to graded impairment of normal dilatory response of the coronary arteries to endothelium-dependent vasodilators and ultimately vasospasm. Furthermore, in animal models it has been shown that low WSS promotes atherosclerotic plaque progression by increasing endothelial low-density lipoprotein uptake and synthesis (39), up-regulating the expression of growth factors and endothelin, down-regulating the expression of growth inhibitors (e.g., transforming growth factor-β) (30,40), and enhancing the proinflammatory gene expression through the mitogen-activated protein kinase and nuclear factor-kappa B pathway (41,42).

Whether these cellular and experimental observations relating low WSS to numerous proatherosclerotic pathways are relevant in human coronary atherosclerosis was previously unknown. We demonstrate that coronary segments with low WSS demonstrate greater absolute vasoconstriction in response to Ach compared with segments with intermediate and high WSS. Our finding that, even after adjusting for demographic and clinical risk factors, low WSS is a strong predictor of severe EDFx, with an odds ratio of 9.14, higher than that of diabetes (5.01) and female sex (2.44), provides a strong underpinning of the association between low WSS with severe EDFx in patients with nonobstructive CAD. Moreover, we show that the probability of severe EDFx increases with decrease in WSS and a value of <1 Pa is could be used to identify segments with severe EDFx.

**COLOCALIZATION OF EDFx AND LOW WSS.** Our study demonstrates that a significantly greater number of segments with severe EDFx reside in low WSS areas. Furthermore, none of the segments with normal endothelial function colocalize with low WSS. Although it is known that WSS patterns are largely driven by regional vascular geometry (low WSS in inner curvature of vessels, outer hips of bifurcations, and upstream and downstream from stenoses), the vascular response to Ach infusion is likely not primarily driven by geometry. Indeed, endothelial responses to Ach are heterogeneous in the same patient despite exposure of all vessel segments to the same systemic risk factors (9,11,12). These data demonstrate the complex interplay between WSS and endothelial function in the presence of nonobstructive CAD.

**FIGURE 3 Distribution of Segments With EDFx**

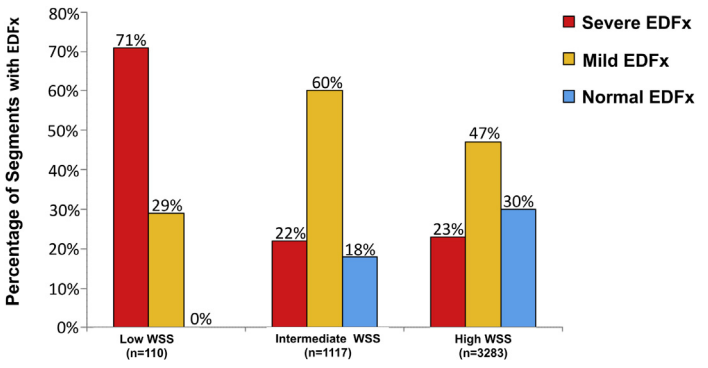


Bar graphs represent the percentage distribution of segments with severe endothelial dysfunction (EDFx), mild EDFx, and normal endothelial function in segments with low, intermediate, and high wall shear stress (WSS).

Prognostic data demonstrate that low WSS is associated with coronary plaque progression (1,3,4) and that patients with EDFx have adverse cardiovascular events. Future studies evaluating the relative predictive value of regional EDFx and WSS with respect to plaque progression and clinical events are warranted.

**CLINICAL IMPLICATIONS.** This study demonstrates that an important regional precursor of coronary plaque progression namely, low WSS, is independently associated with severe EDFx, the final common pathway through which cardiovascular risk factors contribute to atherosclerosis. Interestingly, majority of coronary segments with low WSS had severe EDFx. Although it is known the patients with severe coronary EDFx have adverse cardiovascular

**TABLE 3 Association Between Severe Endothelial Dysfunction and Low Wall Shear Stress Using Logistic Regression Analysis With Generalized Estimating Equations to Account for Within-Subject Correlations**

| | Univariate Models | | Multivariable Model | |
|---|---|---|---|---|
| | Odds Ratio Estimate (95% CI) | p Value | Odds Ratio Estimate (95% CI) | p Value |
| Age (yrs) | 1.02 (0.98–1.05) | 0.30 | 0.99 (0.96–1.03) | 0.80 |
| Female | 2.39 (1.00–5.71) | 0.51 | 2.44 (1.04–5.72) | 0.04 |
| African American | 0.84 (0.35–2.02) | 0.70 | 0.80 (0.38–2.12) | 0.80 |
| Hypertension | 1.19 (0.48–2.97) | 0.71 | 1.33 (0.45–3.94) | 0.60 |
| Diabetes mellitus | 4.44 (2.84–6.93) | <0.001 | 5.01 (1.57–16.01) | 0.007 |
| Active smoker | 1.27 (0.46–3.49) | 0.64 | 1.41 (0.37–5.44) | 0.62 |
| Hyperlipidemia | 1.23 (0.51–2.96) | 0.64 | 1.40 (0.58–3.38) | 0.46 |
| Wall shear stress (<1 Pa vs. ≥1 Pa) | 8.42 (4.07–17.42) | <0.001 | 9.14 (2.60–32.11) | <0.001 |

CI = confidence interval.

**FIGURE 4 Colocalization of Segments With Low WSS and EDFx**

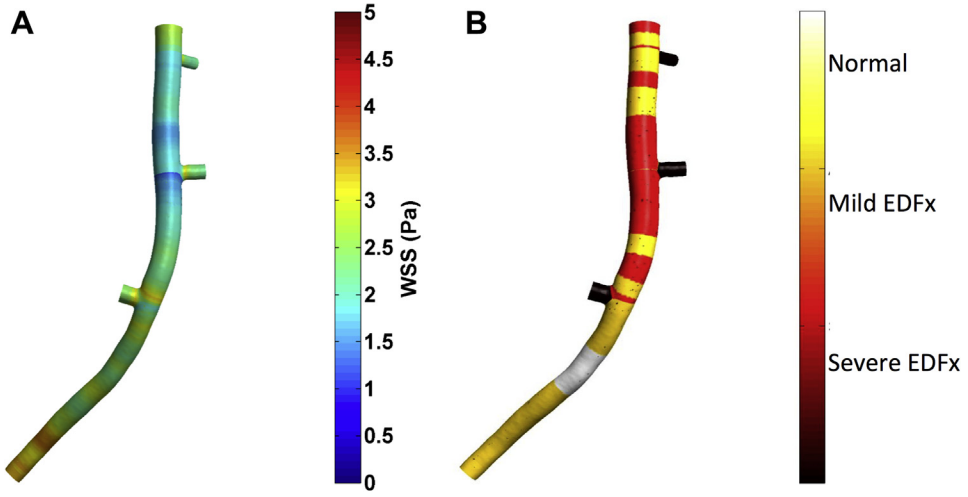


**(A)** A coronary vessel displaying a significant number of segments with low WSS **(blue)** is shown. The same vessel, assessed post-acetylcholine infusion, contains a high number of segments with severe EDFx **(red)** or mild EDFx **(yellow)** in the same regions as baseline low WSS. **(B)** Notice that no segment with normal endothelial function **(white)** colocalizes with low WSS. Abbreviations as in Figure 3.

outcomes and that coronary segments with low WSS are associated with plaque progression, the long-term outcomes of coronary segments that display both EDFx and low WSS are not known (1,43). Future studies are warranted to investigate the prognostic value of such coronary segments. Another opportunity with such detailed physiologic phenotyping of patients is to refine our diagnosis of patients with ongoing chest pain, ischemia, and nonobstructive CAD. Indeed, almost two-thirds of patients with nonobstructive CAD and persistent chest pain with or without a positive stress tests have evidence of coronary EDFx (44). Whether patients with severe EDFx and evidence of segmental low WSS should undergo more intense risk factor modification, antiatherosclerotic or anti-inflammatory therapies remains to be investigated.

**FIGURE 5 Estimated Relationship Between WSS and EDFx Using a Generalized Additive Mixed Model**

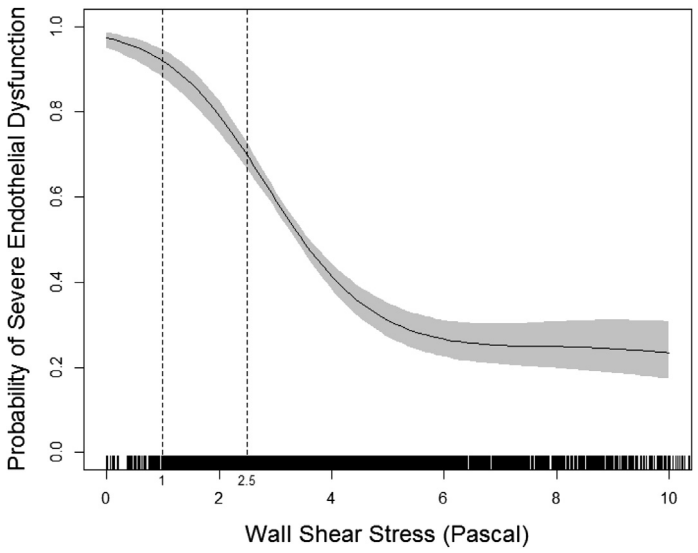


The x-axis indicates WSS in Pascals, along with the number of observations shown; the y-axis indicates the estimated probability of severe EDFx. **Shaded area** represents 95% confidence interval. Abbreviations as in Figure 3.

**STUDY STRENGTHS AND LIMITATIONS.** A strength of our analysis is the methodology of WSS calculation using 3D reconstruction, patient specific pulsatile flow, and boundary conditions imposed on the computational fluid dynamics simulations. The 3D quantitative coronary angiography (QCA) methodology used has been shown to be more accurate than 2-dimensional QCA (conventional single-vessel QCA) measurements (45–48). Although accurate coregistration of 3D WSS values and 2-dimensional QCA-derived diameter measurements for endothelial function assessment is usually challenging, in the present study both these variables were derived from the same 3D-reconstructed geometry, allowing for seamless integration and analysis of the data. Furthermore, once the 3D models were reconstructed, all subsequent operations on surfaces and meshes (centerlines computation, longitudinal

discretization) were fully automated, strengthening the reproducibility of the proposed investigation.

A number of limitations require consideration when interpreting the results of the present study. First, the described relationship between WSS and EDFx does not imply cause and effect, but rather an association. However, the vascular biological underpinnings of both disturbed WSS and EDFx are well established and elucidating the mechanistic links between these 2 variables was not the goal of this investigation. Second, correlated error is introduced by the clustering of numerous arterial segments within patients; however, appropriate statistical methods were used to adjust for correlated error. Third, although both WSS and endothelial function data were derived from the same 3D-reconstructed geometries, inherent inaccuracies due to vessel foreshortening can occur during post-processing of the cineangiograms. We have attempted to minimize these errors through stringent quality control, including comparison of vessel lengths at each clearly demarcated branch point, reconstruction using different views and angles, and standard operating protocols. Furthermore, as per our prespecified protocol, majority of the vessels included in the study were left anterior descending artery, future studies could investigate the relationship between low WSS and severe EDFx in the right coronary artery. In addition, prospective multicentric studies investigating the impact of low WSS and EDFx on clinical outcomes can add provide further insights to the results of our study. Last, although we observed that diabetes associated with severe EDFx even after accounting for data clustering, with only 1 patient with diabetes in our dataset, we had limited ability to test this association.

## CONCLUSIONS

Among patients with nonobstructive CAD, segments with low WSS demonstrated more vasoconstriction in response to Ach than did intermediate or high WSS segments. Low WSS was independently associated with severe EDFx. A value of <1 Pa had the highest estimated probability of severe EDFx.

**ACKNOWLEDGMENTS** The authors thank the Emory interventional cardiology fellows and catheterization staff for participation in the study performance.

**ADDRESS FOR CORRESPONDENCE:** Dr. Habib Samady, Andreas Gruentzig Cardiovascular Center, Division of Cardiology, Department of Medicine, Emory University School of Medicine, 1364 Clifton Road, Suite F606, Atlanta, Georgia 30322. E-mail: hsamady@emory.edu.

## PERSPECTIVES

**WHAT IS KNOWN?** WSS has been shown to play a role in atherogenesis, possibly through endothelial cells. EDFx occurs early in the development of atherosclerosis.

**WHAT IS NEW?** Results of our study show that low WSS plays an important role in the development of severe EDFx.

**WHAT IS NEXT?** Further, coronary segments with low WSS demonstrated a net vasoconstrictive response to acetylcholine. Because EDFx is associated with atherosclerosis, further large prospective studies elucidating the association between WSS and EDFx, and importantly developing WSS as a clinical tool to risk stratify patients with early atherosclerosis, are required.

## REFERENCES

**1.** Samady H, Eshtehardi P, McDaniel MC, et al. Coronary artery wall shear stress is associated with progression and transformation of atherosclerotic plaque and arterial remodeling in patients with coronary artery disease. Circulation 2011;124:779–88.

**2.** Corban MT, Eshtehardi P, Suo J, et al. Combination of plaque burden, wall shear stress, and plaque phenotype has incremental value for prediction of coronary atherosclerotic plaque progression and vulnerability. Atherosclerosis 2014;232:271–6.

**3.** Stone PH, Coskun AU, Kinlay S, et al. Effect of endothelial shear stress on the progression of coronary artery disease, vascular remodeling, and in-stent restenosis in humans: in vivo 6-month follow-up study. Circulation 2003;108:438–44.

**4.** Stone PH, Saito S, Takahashi S, et al. Prediction of progression of coronary artery disease and clinical outcomes using vascular profiling of endothelial shear stress and arterial plaque characteristics: the PREDICTION Study. Circulation 2012;126:172–81.

**5.** Eshtehardi P, McDaniel MC, Suo J, et al. Association of coronary wall shear stress with atherosclerotic plaque burden, composition, and distribution in patients with coronary artery disease. J Am Heart Assoc 2012;1:e002543.

**6.** Hung OY, Brown AJ, Ahn SG, Veneziani A, Giddens DP, Samady H. Association of Wall Shear Stress with Coronary Plaque Progression and Transformation. Interventional Cardiology Clinics 2015;4:491–502.

**7.** Eshtehardi P, Brown AJ, Bhargava A, et al. High wall shear stress and high-risk plaque: an emerging concept. Int J Cardiovasc Imaging 2017;33:1089–99.

**8.** Quyyumi AA, Dakak N, Andrews NP, et al. Nitric oxide activity in the human coronary circulation. Impact of risk factors for coronary atherosclerosis. J Clin Invest 1995;95:1747–55.

**9.** Anderson TJ, Gerhard MD, Meredith IT, et al. Systemic nature of endothelial dysfunction in atherosclerosis. Am J Cardiol 1995;75:71B–4B.

**10.** Bonetti PO, Lerman LO, Lerman A. Endothelial dysfunction: a marker of atherosclerotic risk. Arterioscler Thromb Vasc Biol 2003;23:168–75.

**11.** Prasad A, Zhu J, Halcox JP, Waclawiw MA, Epstein SE, Quyyumi AA. Predisposition to atherosclerosis by infections: role of endothelial dysfunction. Circulation 2002;106:184–90.

**12.** Quyyumi AA. Endothelial function in health and disease: new insights into the genesis of cardiovascular disease. Am J Med 1998;105:32S–9S.

**13.** Brown AJ, Teng Z, Evans PC, Gillard JH, Samady H, Bennett MR. Role of biomechanical forces in the natural history of coronary atherosclerosis. Nat Rev Cardiol 2016;13:210–20.

**14.** Timmins LH, Molony DS, Eshtehardi P, et al. Focal association between wall shear stress and clinical coronary artery disease progression. Ann Biomed Eng 2015;43:94–106.

**15.** Antiga L, Steinman DA. Robust and objective decomposition and mapping of bifurcating vessels. IEEE Trans Med Imaging 2004;23:704–13.

**16.** Piccinelli M, Veneziani A, Steinman DA, Remuzzi A, Antiga L. A framework for geometric analysis of vascular structures: application to cerebral aneurysms. IEEE Trans Med Imaging 2009; 28:1141–55.

**17.** Suwaidi JA, Hamasaki S, Higano ST, Nishimura RA, Holmes DR Jr., Lerman A. Long-term follow-up of patients with mild coronary artery disease and endothelial dysfunction. Circulation 2000;101:948–54.

**18.** Wei J, Mehta PK, Johnson BD, et al. Safety of coronary reactivity testing in women with no obstructive coronary artery disease: results from the NHLBI-sponsored WISE (Women's Ischemia Syndrome Evaluation) study. J Am Coll Cardiol Intv 2012;5:646–53.

**19.** Hambrecht R, Wolf A, Gielen S, et al. Effect of exercise on coronary endothelial function in patients with coronary artery disease. N Engl J Med 2000;342:454–60.

**20.** Takumi T, Yang EH, Mathew V, et al. Coronary endothelial dysfunction is associated with a reduction in coronary artery compliance and an increase in wall shear stress. Heart 2010;96: 773–8.

**21.** Lee BK, Lim HS, Fearon WF, et al. Invasive evaluation of patients with angina in the absence of obstructive coronary artery disease. Circulation 2015;131:1054–60.

**22.** Ku DN. Blood flow in arteries. Annu Rev Fluid Mech 1997;29:399–434.

**23.** Corno AF, Vergara C, Subramanian C, et al. Assisted Fontan procedure: animal and in vitro models and computational fluid dynamics study. Interact Cardiovasc Thorac Surg 2010;10: 679–84.

**24.** Murray CD. The physiological principle of minimum work: I. The vascular system and the cost of blood volume. Proc Natl Acad Sci U S A 1926;12:207–14.

**25.** Murray CD. The physiological principle of minimum work applied to the angle of branching of arteries. J Gen Physiol 1926;9:835–41.

**26.** Hutchins GM, Miner MM, Boitnott JK. Vessel caliber and branch-angle of human coronary artery branch-points. Circ Res 1976;38:572–6.

**27.** Jin S, Oshinski J, Giddens DP. Effects of wall motion and compliance on flow patterns in the ascending aorta. J Biomech Eng 2003;125:347–54.

**28.** Suo J, Oshinski JN, Giddens DP. Blood flow patterns in the proximal human coronary arteries: relationship to atherosclerotic plaque occurrence. Mol Cell Biomech 2008;5:9–18.

**29.** Chatzizisis YS, Baker AB, Sukhova GK, et al. Augmented expression and activity of extracellular matrix-degrading enzymes in regions of low endothelial shear stress colocalize with coronary atheromata with thin fibrous caps in pigs. Circulation 2011;123:621–30.

**30.** Malek AM, Alper SL, Izumo S. Hemodynamic shear stress and its role in atherosclerosis. JAMA 1999;282:2035–42.

**31.** Gimbrone MA Jr., Topper JN, Nagel T, Anderson KR, Garcia-Cardena G. Endothelial dysfunction, hemodynamic forces, and atherogenesis. Ann N Y Acad Sci 2000;902:230–9; discussion 239–40.

**32.** Levesque MJ, Nerem RM. The elongation and orientation of cultured endothelial cells in response to shear stress. J Biomech Eng 1985;107: 341–7.

**33.** Dewey CF Jr., Bussolari SR, Gimbrone MA Jr., Davies PF. The dynamic response of vascular endothelial cells to fluid shear stress. J Biomech Eng 1981;103:177–85.

**34.** Levesque MJ, Liepsch D, Moravec S, Nerem RM. Correlation of endothelial cell shape and wall shear stress in a stenosed dog aorta. Arteriosclerosis 1986;6:220–9.

**35.** Davies PF, Civelek M, Fang Y, Fleming I. The atherosusceptible endothelium: endothelial phenotypes in complex haemodynamic shear stress regions in vivo. Cardiovasc Res 2013;99:315–27.

**36.** Won D, Zhu SN, Chen M, et al. Relative reduction of endothelial nitric-oxide synthase expression and transcription in atherosclerosis-prone regions of the mouse aorta and in an in vitro model of disturbed flow. Am J Pathol 2007;171:1691–704.

**37.** Uematsu M, Ohara Y, Navas JP, et al. Regulation of endothelial cell nitric oxide synthase mRNA expression by shear stress. Am J Physiol 1995; 269:C1371–8.

**38.** Ranjan V, Xiao Z, Diamond SL. Constitutive NOS expression in cultured endothelial cells is elevated by fluid shear stress. Am J Physiol 1995; 269:H550–5.

**39.** Goldstein JL, Kita T, Brown MS. Defective lipoprotein receptors and atherosclerosis. Lessons from an animal counterpart of familial hypercholesterolemia. N Engl J Med 1983;309:288–96.

**40.** Dhawan SS, Avati Nanjundappa RP, Branch JR, et al. Shear stress and plaque development. Expert Rev Cardiovasc Ther 2010;8:545–56.

**41.** Hajra L, Evans AI, Chen M, Hyduk SJ, Collins T, Cybulsky MI. The NF-kappa B signal transduction pathway in aortic endothelial cells is primed for activation in regions predisposed to atherosclerotic lesion formation. Proc Natl Acad Sci U S A 2000;97:9052–7.

**42.** Passerini AG, Polacek DC, Shi C, et al. Coexisting proinflammatory and antioxidative endothelial transcription profiles in a disturbed flow region of the adult porcine aorta. Proc Natl Acad Sci U S A 2004;101:2482–7.

**43.** Jespersen L, Hvelplund A, Abildstrom SZ, et al. Stable angina pectoris with no obstructive coronary artery disease is associated with increased risks of major adverse cardiovascular events. Eur Heart J 2012;33:734–44.

**44.** Sara JD, Widmer RJ, Matsuzawa Y, Lennon RJ, Lerman LO, Lerman A. Prevalence of coronary microvascular dysfunction among patients with chest pain and nonobstructive coronary artery disease. J Am Coll Cardiol 2015;8:1445–53.

**45.** Ishibashi Y, Grundeken MJ, Nakatani S, et al. In vitro validation and comparison of different software packages or algorithms for coronary bifurcation analysis using calibrated phantoms: implications for clinical practice and research of bifurcation stenting. Catheter Cardiovasc Interv 2015;85:554–63.

**46.** Tu S, Huang Z, Koning G, Cui K, Reiber JH. A novel three-dimensional quantitative coronary angiography system: in-vivo comparison with intravascular ultrasound for assessing arterial segment length. Catheter Cardiovasc Interv 2010; 76:291–8.

**47.** Tu S, Xu L, Ligthart J, et al. In vivo comparison of arterial lumen dimensions assessed by co-registered three-dimensional (3D) quantitative coronary angiography, intravascular ultrasound and optical coherence tomography. Int J Cardiovasc Imaging 2012;28:1315–27.

**48.** Tuinenburg JC, Janssen JP, Kooistra R, et al. Clinical validation of the new T- and Y-shape models for the quantitative analysis of coronary bifurcations: an interobserver variability study. Catheter Cardiovasc Interv 2013;81:E225–36.

**KEY WORDS** computational fluid dynamics, coronary wall shear stress, endothelial dysfunction, nonobstructive coronary artery disease

**APPENDIX** For an expanded Methods section, please see the online version of this paper.